

A Graph Approach to Dynamic Fractional Frequency Reuse (FFR) in Multi-Cell OFDMA Networks

Ronald Y. Chang[†], Zhifeng Tao[◇], Jinyun Zhang[◇] and C.-C. Jay Kuo[†]

[†] Ming Hsieh Department of Electrical Engineering and Signal and Image Processing Institute
University of Southern California, Los Angeles, CA 90089-2564, USA

[◇] Mitsubishi Electric Research Labs (MERL), Cambridge, MA 02139, USA

E-mail: yjrchang@gmail.com, tao@merl.com, jzhang@merl.com and cckuo@sipi.usc.edu

Abstract—A graph-based framework for dynamic fractional frequency reuse (FFR) in multi-cell OFDMA networks is proposed in this work. FFR is a promising resource allocation technique that can effectively mitigate inter-cell interference (ICI) in OFDMA networks. The proposed scheme enhances the conventional FFR by enabling adaptive spectral sharing per cell load conditions. Such adaptation has significant benefits in a practical environment where traffic load in different cells may be asymmetric and time-varying. The dynamic feature is accomplished via a graph approach in which the resource allocation problem is translated to a graph coloring problem. Specifically, in order to incorporate various versions of FFR in our framework, we construct a graph that matches the specific version of FFR and then color the graph using the corresponding graph algorithm. The performance improvement enabled by the proposed dynamic FFR scheme is further demonstrated by computer simulation for a 19-cell network with asymmetric cell load. For instance, the proposed dynamic FFR scheme can achieve a 12% and 33% gain in cell throughput and service rate over conventional FFR, and render a 70% and 107% gain in cell throughput and service rate with respect to the reuse-3 system.

I. INTRODUCTION

Thanks to its effectiveness and flexibility in radio resource allocation, as well as its capability of combating frequency selective fading, Orthogonal Frequency Division Multiple Access (OFDMA) has become widely adopted in many next-generation cellular systems such as 3GPP Long Term Evolution (LTE) [1] and IEEE 802.16m [2] advanced WiMAX. Since radio spectrum has long been deemed the most scarce resource, advanced radio resource management (RRM) scheme that can increase the OFDMA network capacity and reduce the deployment cost has been in dire demand. The need for such an RRM algorithm becomes even more acute today, as the number of subscribers continues to experience unprecedented growth globally and the amount of sheer volume of traffic increases incessantly.

One conventional approach to improving spectrum efficiency is to reuse the same frequency band in multiple geographical areas or cells. However, inter-cell interference (ICI) will be inevitably incurred, when users or mobile stations (MSs) in *adjacent* cells share the same spectrum. Since ICI is the major performance-limiting issue in wireless cellular

networks [3], a good interference management (IM) scheme that can mitigate ICI is a central part of RRM.

The simplest IM scheme is the reuse- n ($n > 1$) system, where any two adjacent cells use different channels and thus no MS will cause any pronounced interference to MSs in adjacent cells. Such system, however, tends to lose more bandwidth efficiency than what can be gained in signal quality improvement enabled by ICI reduction. Thus, recent research activities have outlined several improved IM schemes for the next generation OFDMA systems. Fractional frequency reuse (FFR), for instance, is such a technique supported in WiMAX. FFR is designed with the goal of striking a better trade-off between spectral efficiency (*i.e.*, advantage of supporting more users) and interference mitigation (*i.e.*, advantage of improving signal-to-interference-noise ratio (SINR)) by leveraging the largely different experience of ICI at cell-center and cell-edge MSs. In particular, since cell-edge MSs are more ICI-prone than cell-center MSs, MSs in cell center essentially have a smaller reuse factor (*e.g.*, $n = 1$) while MSs at cell edge are granted with a bigger reuse factor (*e.g.*, $n = 3$).

FFR has drawn significant research attention due to its efficiency. Examples and applications of FFR were discussed in [4]–[6]. A variation of FFR was proposed in [7] where a cell is partitioned into several concentric regions, and smaller reuse factor is assigned to inner regions while bigger reuse to outer regions. However, all these schemes are of fixed configuration. In other words, their spectrum allocation is predetermined and cannot adjust adaptively according to the dynamic cell load variations. Unfortunately, this rigidity of fixed FFR will result in inefficient spectral usage, as MSs in heavy-load areas may suffer from insufficient spectrum resource while those in light traffic areas can not use the allocated frequency channel fully.

In this work, we propose a dynamic FFR scheme that can adapt to the dynamic cell load. Our scheme can balance cell load and attain higher overall cell throughput by means of redistributing the radio resource among cells with unequal load. This adaptation is realized by a novel graph approach where FFR is first mapped to an interference graph and then solved by proper coloring on the graph. Various versions of FFR can be incorporated into this framework easily.

II. SYSTEM DESCRIPTION

We consider a downlink cellular system with L base stations (BSs), each serving $M^{(l)}$ MSs, $l = 1, 2, \dots, L$, and $\sum_{l=1}^L M^{(l)} = M$. A set of N subchannels is available for resource allocation. The downlink signal for MS m is sent with power P_m , depending on its proximity to the BS. Specifically, we have

$$P_m = \begin{cases} P_0, & \text{if MS } m \text{ is in cell center,} \\ P_1, & \text{if MS } m \text{ is on cell edge,} \end{cases} \quad (1)$$

and $P_0 < P_1$. The boundary that separates the cell center and the cell edge is a design parameter. The transmitted signal then undergoes slow fading (i.e., path loss) as well as fast fading (i.e., Rayleigh fading) before it reaches the target MS. Let $\varphi_m^{(l)}$ be the path loss attenuation factor from BS l to MS m , and $\beta_{mn}^{(l)}$ the fast fading channel power in subchannel n , from BS l to MS m . Thus, the received signal power at MS m from BS l in subchannel n is given by $P_m \beta_{mn}^{(l)} \varphi_m^{(l)}$.

We consider a typical scenario where each MS m is registered at and communicates with one BS, which is called the anchor (or serving) BS and denoted as A_m . The signal-to-interference-and-noise ratio (SINR) is used to evaluate the performance of a multi-cell wireless cellular network as it is a more accurate measure than SNR in interference-limited environments. In the downlink scenario, the SINR (in the linear scale) of the received signal at MS m using subchannel n is given by

$$\text{SINR}_{m,n} = \frac{P_m \beta_{mn}^{(A_m)} \varphi_m^{(A_m)}}{\sum_{v \in \mathbb{I}_m} P_v \beta_{mn}^{(A_v)} \varphi_m^{(A_v)} + N_0 W}, \quad (2)$$

where \mathbb{I}_m is the set of interfering MSs, N_0 is the thermal noise density, and W is the subchannel bandwidth.

While SINR is a useful evaluation metric for individual quality of service, cell throughput can better represent the overall performance of different IM schemes. Also, as some IM schemes such as the reuse- n and FFR only grant service to limited users within its capacity, it is of interest to understand the service rate, or the percentage of MSs being served, in different IM schemes. We quantify these two performance measures mathematically in the following. Let $\mathbb{S}^{(l)}$ be the set of MSs that are being served in cell l . Assume that a served MS m , $m \in \mathbb{S}^{(l)}$, is allocated a single subchannel $c_m^{(l)} \in \{1, 2, \dots, N\}$. Then, the theoretical cell throughput (bits/sec) for cell l is given by the capacity formula:

$$T^{(l)} = \sum_{m \in \mathbb{S}^{(l)}} W \log_2(1 + \text{SINR}_{m,c_m^{(l)}}). \quad (3)$$

The service rate in cell l is simply:

$$G^{(l)} = \frac{|\mathbb{S}^{(l)}|}{M^{(l)}}, \quad (4)$$

where $|\mathbb{S}^{(l)}|$ is the cardinality of the set $\mathbb{S}^{(l)}$, and we assume all $M^{(l)}$ MS in a cell always have traffic to transceive. A good IM scheme will manage the resource allocation so that more users are served (large $G^{(l)}$) and, in the meantime, good quality of

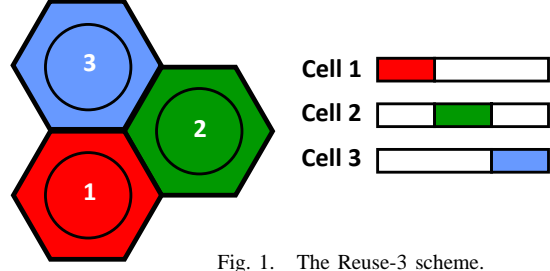


Fig. 1. The Reuse-3 scheme.

service is guaranteed for these users to amount to a high total throughput (large $T^{(l)}$).

III. PREVIOUS INTERFERENCE MANAGEMENT SCHEMES

In this section, we introduce several interference management (IM) schemes that are related to our work.

A. Reuse-3

The simplest IM scheme is a reuse- n ($n > 1$) system. A reuse- n system partitions a geographical area into n regions, each of which is exclusively allocated a band¹ in such a way that cells physically close to each other are assigned with different bands to avoid dominant ICI. Cells that are sufficiently far from each other may reuse the same band, and how frequently (in space) such reuse is practiced is dictated by the reuse factor n . For instance, $n = 3$ if the same band is reused every three cells. A Reuse-3 ($n = 3$) scheme is depicted in Fig. 1, showing three neighboring cells which use orthogonal bands each equal to one-third of the total bandwidth. The three-cell scheme shown here is the basic building blocks for any size of the geographical area, and thus the principle can be easily generalized to more cells. In fact, in a typical Reuse-3 deployment, each cell will be surrounded by six immediate neighboring cells that occupy a band different from that of the center cell. This eliminates strongest ICI at the cost of reduced spectral efficiency as only one-third of the bandwidth is used in each cell.

B. FFR-A

The generic frequency reuse approach faces the trade-off between spectral efficiency that can be achieved by small n and interference mitigation that can be accomplished by big n . For instance, the aforementioned Reuse-3 scheme trades the spectral efficiency for the benefit of complete nullification of interference from first-tier cells. The challenge of finding an appropriate sweet-spot spurs the development of a more flexible frequency reuse scheme, notably, the FFR.

FFR may be realized in many fashions. One realization, termed FFR-A in this work, is shown in Fig. 2. FFR-A suggests that the cell center of neighboring cells share the same band, while their cell edge are separate on orthogonal bands. Besides, the cell-center and cell-edge bands in neighboring cells are non-overlapping. The color on the spectrum is shown to match the color of the geographical area. The white color in Fig. 2 indicates the portion of the spectrum that is refrained from use so that the cell-edge orthogonality can be maintained.

¹We use *band* and *spectrum* interchangeably in this paper.

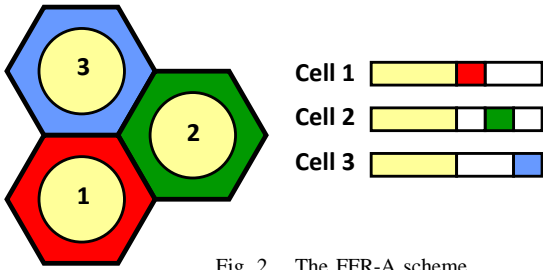


Fig. 2. The FFR-A scheme.

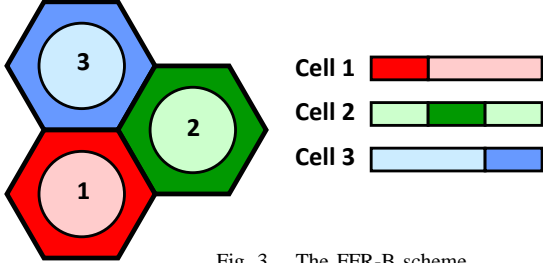


Fig. 3. The FFR-B scheme.

C. FFR-B

A different realization of FFR, termed FFR-B, is shown in Fig. 3. FFR-B, different from FFR-A, allows partial overlapping between cell-center and cell-edge bands in neighboring cells. Consequently, there is no part of the spectrum that must not be used (“white color”), as the cell-edge orthogonality can still be maintained by filling in the “white spectrum” with the cell center users. This gives FFR-B both pros and cons; *i.e.*, while FFR-B enjoys higher spectral efficiency it has higher ICI caused between cell-center and cell-edge MSs of the neighboring cells.

To facilitate discussion in the later sections, we introduce two notations to indicate the cell-center and cell-edge bands. Let $\mathbb{O}_i^{(u)}$ (or $\mathbb{P}_i^{(u)}$) be the band allocated to the cell center (or the cell edge) of cell i for the scheme u , where $i = 1, 2, 3$ and $u = R, A, B$ representing Reuse-3, FFR-A and FFR-B schemes, respectively. Note that a band may or may not be a contiguous frequency spectrum.

IV. PROPOSED DYNAMIC FFR SCHEMES USING THE GRAPH APPROACH

The channel assignment problem in cellular and mesh networks has been studied in the context of multi-coloring of a graph for decades (see, *e.g.*, [8]). In the traditional formulation, each node in a graph corresponds to a BS or an access point (AP) in the network to which channels are assigned. The edge connecting two nodes represents the co-channel interference in between, which typically corresponds to the geographical proximity of these two nodes. Then, the channel assignment problem becomes the node coloring problem, where two interfering nodes should not have the same color, *i.e.*, use the same channel.

Recently, this graph approach finds its application in reuse-1 OFDMA networks [9]. In this new application, the node in the graph corresponds to an MS instead of a BS since the target of the channel assignment is now the MSs. The method

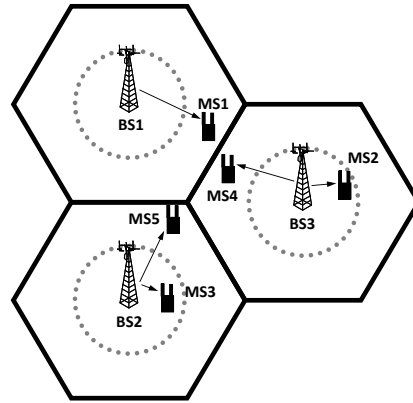


Fig. 4. An exemplary multi-cell, multi-user scenario.

TABLE I
THE GRAPH CONSTRUCTION RULE FOR FFR-A

Node a and node b in the interference graph are connected by an edge if:

- A1. MS a and MS b are users of the same cell; or
- A2. MS a is a cell-edge user of cell i and MS b is a cell-edge user of cell j , where cell i and cell j are neighbors^a; or
- A3. MS a is a cell-center user of cell i and MS b is a cell-edge user of cell j , or, MS a is a cell-edge user of cell i and MS b is a cell-center user of cell j , where cell i and cell j are neighbors.

Otherwise, node a and node b are not connected by an edge.

^aTwo cells are *neighbors* if they are physically adjacent to each other. In a typical hexagonal deployment, a cell has six neighbors.

presented in [9], however, can not be directly applied to non-reuse-1 OFDMA systems. Thus, for the graph framework to be useful for FFR-A and FFR-B considered in this work, we must design a new method. Towards this end, we develop a new graph construction strategy and a coloring method to achieve dynamic FFR-A and FFR-B that can adapt to dynamic cell load changes.

A. Graph Construction Strategy

The first step in the graph-based approach is to construct an interference graph, which is comprised of nodes representing MSs and edges representing the interference between two MSs. Whether two nodes are connected by an edge (or, equivalently, two MSs are considered interfering) is determined by the topology of MSs as well as the adopted IM scheme. For instance, since FFR-A and FFR-B in Figs. 2 and 3 have different resource allocation strategies, they also have different interference graphs.

The graph construction rule for FFR-A is described in Table I. Two nodes are connected by an edge if they satisfy specific pairwise relations. Specifically, pairs of nodes have edges if they have intra-cell relationship (A1) or particular inter-cell relationships (A2 and A3) which, according to FFR-A, poses some channel assignment (or, in the graph, coloring) constraints. These inter-cell constraints include the use of non-overlapping bands for cell-edge/cell-edge (A2) and cell-

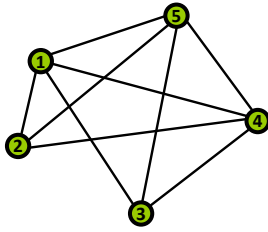


Fig. 5. The interference graph constructed for the FFR-A scheme corresponding to the multi-cell, multi-user scenario in Fig. 4.

TABLE II

THE GRAPH CONSTRUCTION RULE FOR FFR-B

Node a and node b in the interference graph are connected by an edge if:

- B1. MS a and MS b are users of the same cell; or
- B2. MS a is a cell-edge user of cell i and MS b is a cell-edge user of cell j , where cell i and cell j are neighbors.

Otherwise, node a and node b are not connected by an edge.

center/cell-edge (A3) users of neighboring cells. Since two cell-center MSs of neighboring cells are permitted to use overlapping bands in FFR-A, corresponding nodes are not connected by an edge.

Consider applying the graph construction rule in Table I to an illustrative scenario with 3 BSs and 5 MSs as shown in Fig. 4. After pairwise examination, the resulting interference graph is drawn in Fig. 5. Note that all pairs of nodes satisfy A1–A3 relations and therefore are connected by an edge, except for nodes 2 and 3, which are not connected by an edge because MSs 2 and 3 are cell-center users of different cells.

The graph construction rule for FFR-B is described in Table II. Again, pairs of nodes have edges if they have intra-cell relationship (B1) or particular inter-cell relationship (B2). Different from FFR-A, however, the inter-cell constraints posed by FFR-B include only the use of non-overlapping bands for cell-edge/cell-edge users of neighboring cells (B2).

The interference graph constructed for FFR-B corresponding to the scenario in Fig. 4 is drawn in Fig. 6. Note that the graph for FFR-B has fewer edges. This is due to less inter-cell constraints as discussed previously.

B. Graph Coloring Algorithm

The second step in the graph-based approach is to color the nodes in the interference graph. A color corresponds to a subchannel, and the coloring of nodes is equivalent to the channel allocation to the MSs. A coloring is considered proper if the “coloring constraint” is met: any two neighboring nodes (*i.e.*, nodes connected by an edge) in the graph are assigned with different colors.

Many coloring algorithms have been proposed to color a graph efficiently. Most of the algorithms, including the Brélaž’s algorithm [10], were proposed to color a graph given the graph is colorable. In other words, sufficient colors are provided for coloring the graph. In the graph for an OFDMA

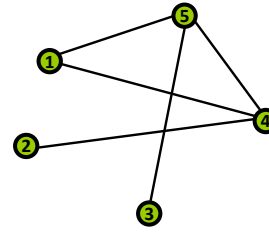


Fig. 6. The interference graph constructed for the FFR-B scheme corresponding to the multi-cell, multi-user scenario in Fig. 4.

TABLE III

THE MODIFIED BRÉLAZ’S ALGORITHM FOR COLORING GRAPHS

1. Select from the unexamined subgraph (or initially, the entire graph) a node x whose available color set, $a(x)$, is of minimum size. The $a(x)$ is defined as the set of colors that may be used to color node x such that the coloring constraint is respected.
2. If there are ties, break ties by selecting one whose degree^e is maximum in the unexamined subgraph. If there are still ties, break ties arbitrarily.
3. Color the selected node x with color randomly selected from $a(x)$. If $a(x)$ is empty, leave the node uncolored.
4. Repeat 1–3 until all nodes are examined.

^eThe *degree* of a node is the number of edges incident to the node.

network, however, this condition may not be fulfilled as the size of the graph will change on the cell load (*i.e.*, the number of MSs) in the network while the number of colors (subchannels) is fixed. When the network is heavily loaded, or colors are under-provided, a new strategy must be introduced into the coloring algorithm to address the fact that coloring the entire graph is not possible. When the network is lightly loaded, or colors are over-provided, it is desirable to balance the use of colors to reduce unnecessary “color collision” (and consequently, channel collision and ICI). In light of the above observations, we propose to modify the Brélaž’s algorithm to meet the above needs in OFDMA networks.

The modified Brélaž’s algorithm is presented in Table III. Nodes are colored successively, one at a time. As in the original Brélaž’s algorithm, we select a node in each iteration from the unexamined subgraph (Steps 1 & 2). Then, this selected node is colored with a color *randomly* selected from the available color set of this node (Step 3), instead of the lowest numbered color in [10]. This helps attain color balancing when colors are over-provided. Besides, when the available color set is empty, as might happen when colors are under-provided, we include the option of leaving the node uncolored (Step 3). The whole procedure is repeated for the next node until all nodes are examined (Step 4); *i.e.*, either colored or, by decision, uncolored.

V. SIMULATION RESULTS

In this section, we study the performance of the proposed schemes by computer simulation.

TABLE IV
SIMULATION SETUP

Cell Parameters	
Number of Cells, L	19
Cell Radius	750 m
Cell-center Radius	500 m
Inter-cell Distance Ratio ^a	0.9
Antennas	SISO
OFDMA Parameters	
Total Bandwidth, Ω	30 MHz
Carrier Frequency	2.5 GHz
Number of Subchannels, N	30
Number of Subcarriers Per Subchannel	28
Channel Model	
Path Loss (dB)	$130.62 + 37.6 \times \log_{10}(d)$, (d in km)
Power Control Parameters	
Cell-center Trans. Power, P_0	40 dBm
Cell-edge Trans. Power, P_1	46 dBm
Thermal Noise Density, N_0	-174 dBm/Hz

^aCell-to-cell distance is used to control cell overlapping area. The ratio shown here is relative to the hexagonal back-to-back cell deployment.

A. Simulation Setup

The simulation setup follows closely the suggestion given for the IEEE 802.16m evaluation [11]. It is summarized in Table IV.

Partitioning the total bandwidth, Ω , into cell-center and cell-edge parts is a design parameter. It is however desirable to consider a partition roughly proportional to the traffic load in cell-center and cell-edge areas. For our current definition of cell-center area as shown in Table IV, we consider the following bandwidth allocation for fixed IM schemes. For fixed Reuse-3, since there is no distinction between the cell-center and the cell-edge, we have $|\mathbb{O}_i^{(R)} \cup \mathbb{P}_i^{(R)}| = \Omega/3, i = 1, 2, 3$. That is, each cell is allocated a fixed 10 MHz bandwidth. For fixed FFR-A, we assume $|\mathbb{O}_i^{(A)}| = \Omega/2$ and $|\mathbb{P}_i^{(A)}| = \Omega/6, i = 1, 2, 3$. For fixed FFR-B, we assume $|\mathbb{O}_i^{(B)}| = 2 \times \Omega/3$ and $|\mathbb{P}_i^{(B)}| = \Omega/3, i = 1, 2, 3$. Note that this allocation corresponds roughly to the illustration in Figs. 1–3. For all fixed schemes, if the service capacity of the allocated band is reached, additional users will not be served.

To allow fair comparison of fixed and dynamic FFR-A, we consider a common partition of the bandwidth into cell-center and cell-edge usage for both schemes. The need of this practice arises as the “white spectrum” in both fixed and dynamic FFR-A must be equalized for fair comparison. Generally, the white or unused spectrum expands as $|\mathbb{O}_i^{(A)}|$ shortens. Thus, we adopt the same $|\mathbb{O}_i^{(A)}| = \Omega/2, i = 1, 2, 3$ for both fixed and dynamic FFR-A schemes. Note that FFR-B does not require such practice as it has no “white spectrum” as explained in Sec. III.

B. Results and Discussion

First, we simulate the symmetric load scenario. That is, each cell has an equal number of uniformly distributed MSs. Fig. 7 shows the cell throughput performance, obtained by (3) and averaged over all cells, for five IM schemes in comparison. It is seen that in very low load conditions Reuse-3 outperforms others. This is because Reuse-3 eliminates dominant ICI from all first-tier interferers and has 100% service rate in low load conditions (Fig. 8). In contrast, FFR-A and FFR-B are disadvantaged in very low load scenario due to partial channel collision, which is avoided entirely in Reuse-3. It is also seen that FFR-A outperforms FFR-B in spite of lower service rate (Fig. 8). This is because a served MS has better SINR in FFR-A than in FFR-B due to FFR-A’s tighter band allocation constraints.

As the traffic load increases, Reuse-3 becomes increasingly inefficient as more users are rejected from service, as revealed by the low service rate in Fig. 8 and the stagnant cell throughput in Fig. 7. This inefficiency is however remedied by the FFR. As shown in Fig. 8, FFR-A and FFR-B have much improved service rate, which contributes to the higher cell throughput in Fig. 7. It is also seen that the dynamic FFR-A (FFR-B) achieves slightly better throughput and service rate than the fixed FFR-A (FFR-B), but with largely comparable performance. The advantage of the dynamic scheme is less noticeable in the symmetric load scenario because its capability of redistributing the channel resource among cells can not be fully exploited. The slight improvement achieved by the dynamic scheme in the symmetric load case is mainly contributed from the flexible use of the spectrum which is unavailable in the fixed FFR-A and FFR-B schemes.

Second, we simulate the asymmetric load scenario. We define the *traffic load ratio* as the load proportion of heavy- to light-load cells. For every three cells, we consider two light-load cells and one heavy-load cell, where the light-load cells have a fixed cell load of two MSs and the heavy load cell has a controllable cell load according to the traffic load ratio. We plot the same performance measures for different traffic load ratio in Figs. 9 and 10. It is seen that, in sharp contrast to the symmetric load scenario, the dynamic FFR-A (FFR-B) improves the fixed FFR-A (FFR-B) and the fixed reuse-3 significantly in both cell throughput (Fig. 9) and service rate (Fig. 10). Specifically, when the traffic load ratio is equal to 15, the dynamic FFR-A improves the fixed FFR-A by 12% in cell throughput and 33% in service rate, and improves the fixed reuse-3 system by 70% in cell throughput and 107% in service rate. This is due to the flexibility in borrowing light-load cells’ resource for the use of heavy-load cells in the dynamic scheme. In addition, we observe that the performance improvement of the dynamic FFR-A over the fixed FFR-A is higher than that of the dynamic FFR-B over the fixed FFR-B. This is because the more constrained use in cell-edge band in FFR-A can benefit more from the adaptability yielded by the dynamic operation.

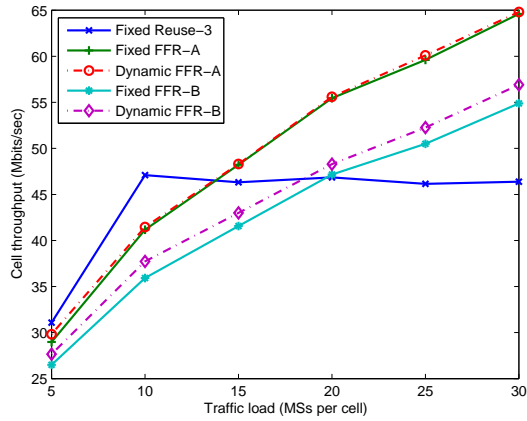


Fig. 7. The cell throughput in symmetric cell load scenarios.

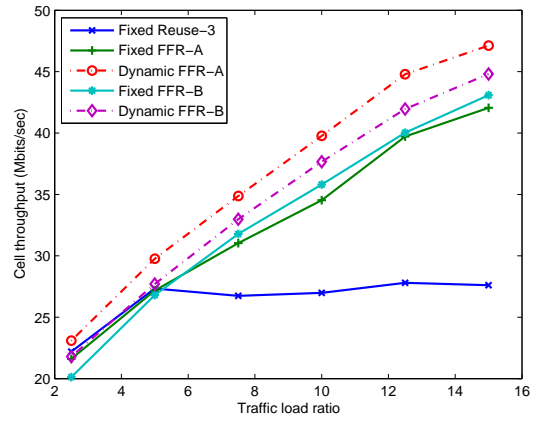


Fig. 9. The cell throughput in asymmetric cell load scenarios.

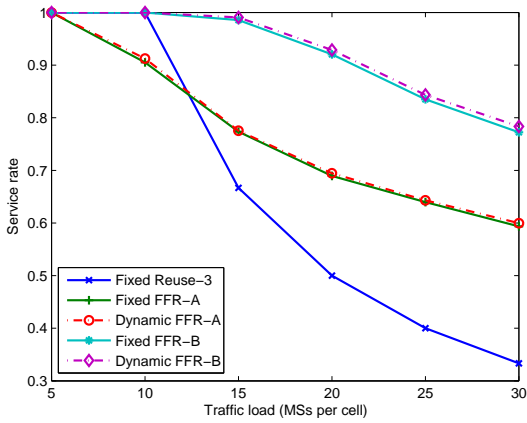


Fig. 8. The service rate in symmetric cell load scenarios.

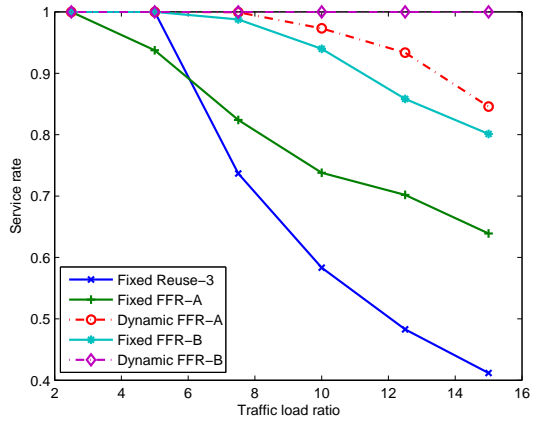


Fig. 10. The service rate in asymmetric cell load scenarios.

VI. CONCLUSION

A dynamic fractional frequency reuse (FFR) framework for multi-cell OFDMA networks was proposed in this work. The dynamic feature is characterized by the capability of adjusting the spectral resource to varying cell load conditions. The adaptation is accomplished via a graph approach in which the resource allocation problem is translated to a graph coloring problem. Different versions of FFR can be easily realized in this framework by customizing the graph to match the specific FFR principle. The proposed dynamic scheme is shown to deliver higher cell throughput and service rate, especially in asymmetric cell load scenarios. Thanks to its practicality, the proposed method can be used in next generation cellular systems such as 3GPP Long Term Evolution (LTE) and IEEE 802.16m.

REFERENCES

- [1] 3GPP Long Term Evolution (LTE). [Online]. Available: <http://www.3gpp.org/Highlights/LTE/LTE.htm>
- [2] IEEE 802.16 Task Group m. [Online]. Available: <http://ieee802.org/16/tgm/>

- [3] I. Katzela and M. Naghshineh, "Channel assignment schemes for cellular mobile telecommunication systems: a comprehensive survey," *IEEE Personal Commun.*, vol. 3, pp. 10–31, June 1996.
- [4] R1-050764, "Inter-cell interference handling for E-UTRA," in *3GPP TSG-RAN WG1 Meeting #42*, Aug. 2005.
- [5] R1-050833, "Interference mitigation in evolved UTRA/UTRAN," in *3GPP TSG-RAN WG1 Meeting #42*, Aug. 2005.
- [6] C.-S. Chiu and C.-C. Huang, "Combined partial reuse and soft handover in OFDMA downlink transmission," in *Proc. IEEE VTC'08*, Apr. 2008, pp. 1707–1711.
- [7] IEEE C802.16m-08/034, "Adaptive frequency reuse for interference management in IEEE 802.16m system," Jan. 2008.
- [8] L. Narayanan, "Channel assignment and graph multicoloring," *Handbook of Wireless Networks and Mobile Computing*, pp. 71–94, 2002.
- [9] Y. Chang, Z. Tao, J. Zhang, and C.-C. J. Kuo, "A graph-based approach to multi-cell OFDMA downlink resource allocation," in *Proc. IEEE GLOBECOM'08*, Nov. 2008.
- [10] D. Brélaz, "New methods to color the vertices of a graph," *Communications of the ACM*, vol. 22, pp. 251–256, Apr. 1979.
- [11] *Draft IEEE 802.16m Evaluation Methodology*. IEEE 802.16 Broadband Wireless Access Working Group, 2007.